Near-field 3D Spherical Active Coded Aperture Gamma-ray Imaging

D. Hellfeld[1], P. Barton[2], L. Mihailescu[2], K. Vetter[1,2]
[1]Department of Nuclear Engineering, University of California, Berkeley
[2]Applied Nuclear Physics, Lawrence Berkeley National Laboratory

INTRODUCTION

Hand-held imagers are efficient search tools as they can overcome the inverse square law by moving much closer to potential sources than traditional static imagers. However, as the system is brought close to the source, near-field effects can begin to dominate and, if not accounted for in the reconstruction, can produce artifacts and additional blurring. By properly characterizing and utilizing the near-field effects, the artifacts can be removed and spatial resolution can be increased. In this work we describe the methods used to characterize the near-field effects in the Portable Radiation Imaging Spectroscopy and Mapping (PRISM) system and the subsequent improvements in 3D imaging, specifically in the low-energy coded aperture reconstruction domain.

PRISM

- Hand-held, free-moving, dual-mode, cm^3 CZT-CPG based omnidirectional spherical active coded aperture.
- Visual camera, LiDAR, and inertial measurement unit (IMU) are attached for real-time contextual sensing and tracking.

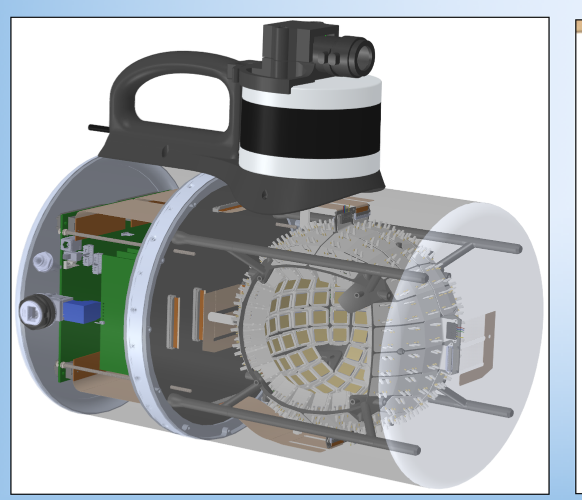
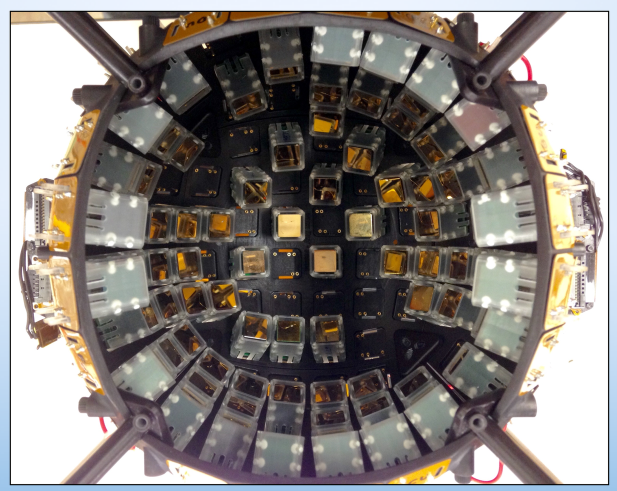
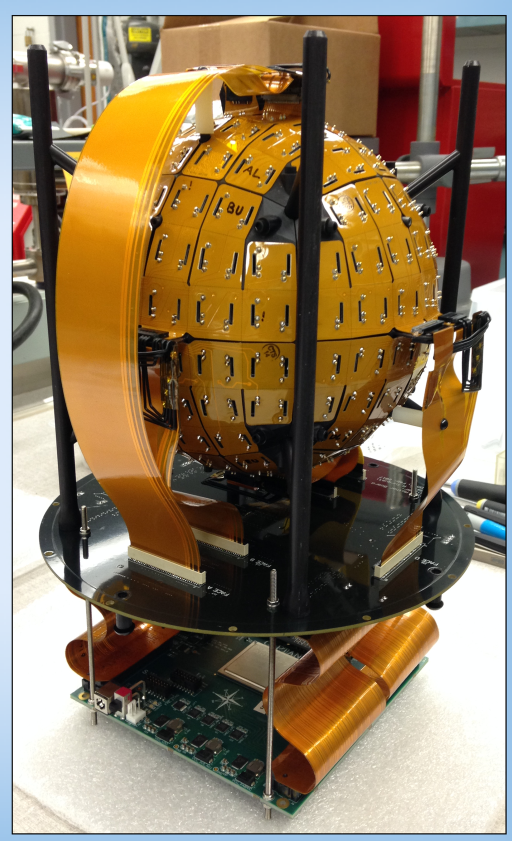

3D IMAGING AND SCENE DATA FUSION

- 3D imaging is achieved by combining data from multiple perspectives while tracking the position and orientation of the system.

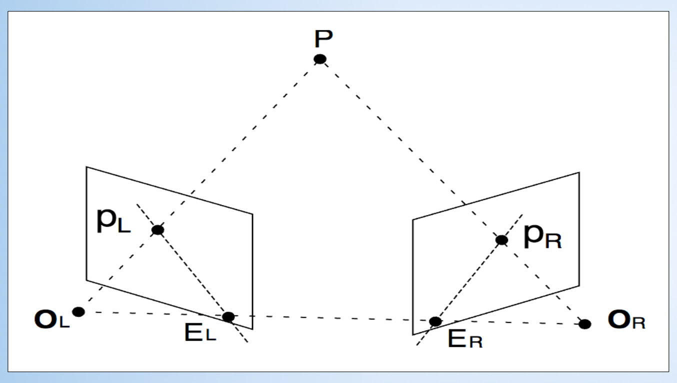

- Contextual data *fused* with 3D γ-ray data to constrain image reconstruction to occupied voxels in the 3D scene model - increasing accuracy and computational efficiency.

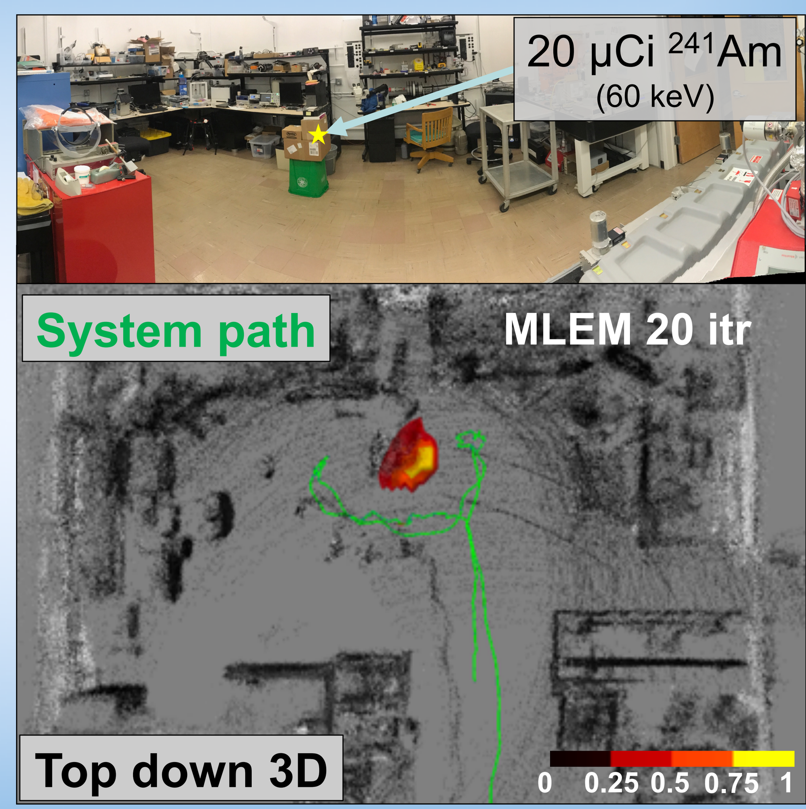

NEAR-FIELD EFFECTS

- As the source is brought closer to the system (< 50-70 cm), magnification and solid angle effects due to finite detector size will dominate and the far-field approximation breaks down.
- Near-field response is simulated at various distances using a zero-energy graphics-based perspective projection approach in OpenGL.
- Detectors are assigned unique 8-bit color values - color histogram of projection to determine effective flux for each direction.

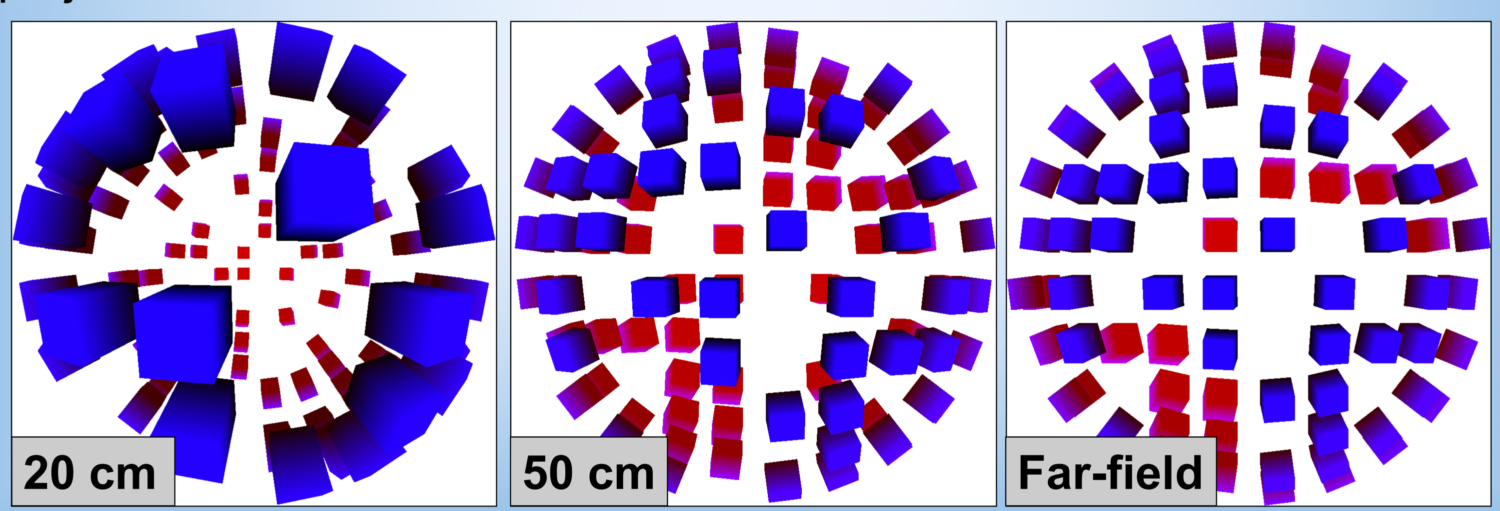

STATIC 3D IMAGING

- 3D imaging possible in the near-field with single static measurement.
- 5-min measurement of 20 µCi ^{241}Am source placed 30 cm from center of sphere.
- Reconstruction with MLEM (75 itr) using far-field (FF), far-field with finite detector (FF-FD), and interpolated near-field (NF) responses.

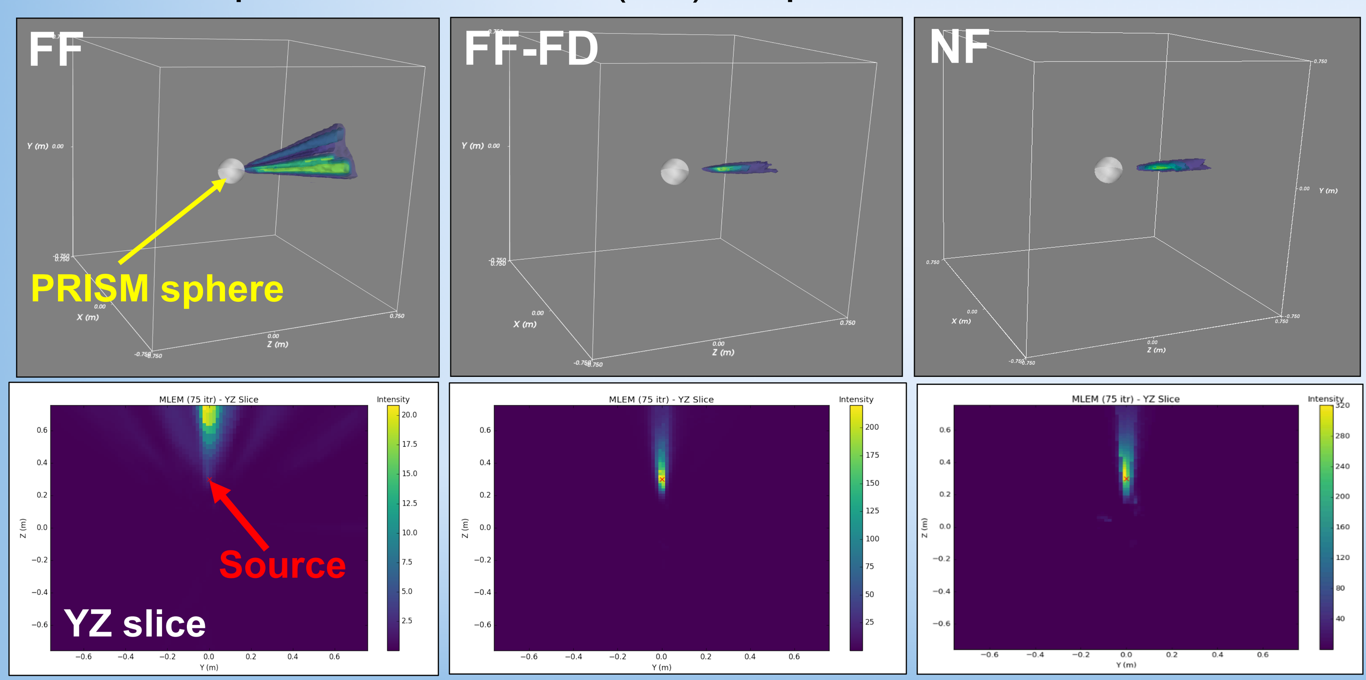

- Depth resolution of FF-FD worse than NF, but may be appropriate for lower computational burden

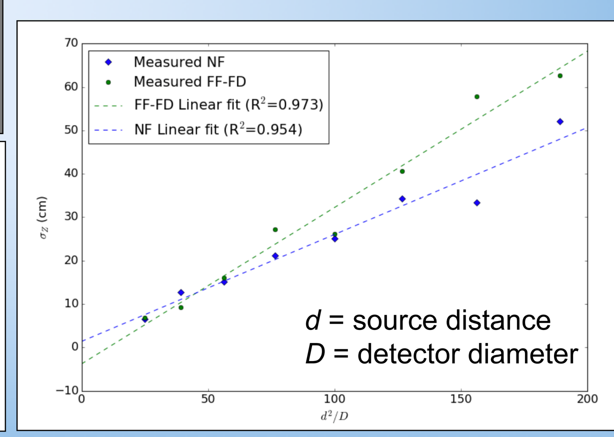

FREE-MOVING 3D IMAGING

- The user setup includes a laptop used for contextual data processing and batteries in a backpack and a hand-held tablet for gamma-ray reconstruction and visualization (**top left**).
- A 20 µCi ^{241}Am source (60 keV) source was placed in a box on lab bench (**top right**)
- After a quick (45 s) pass-through of the scene, a potential source location is found in < 3 s (**bottom left**).
- A longer (1.5 min) near-field measurement is then performed to enhance 3D spatial resolution (**bottom right**).

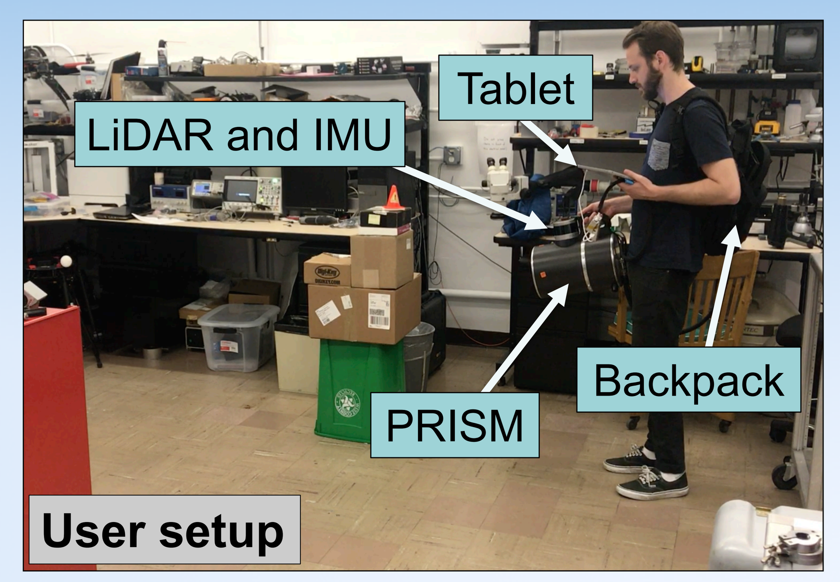

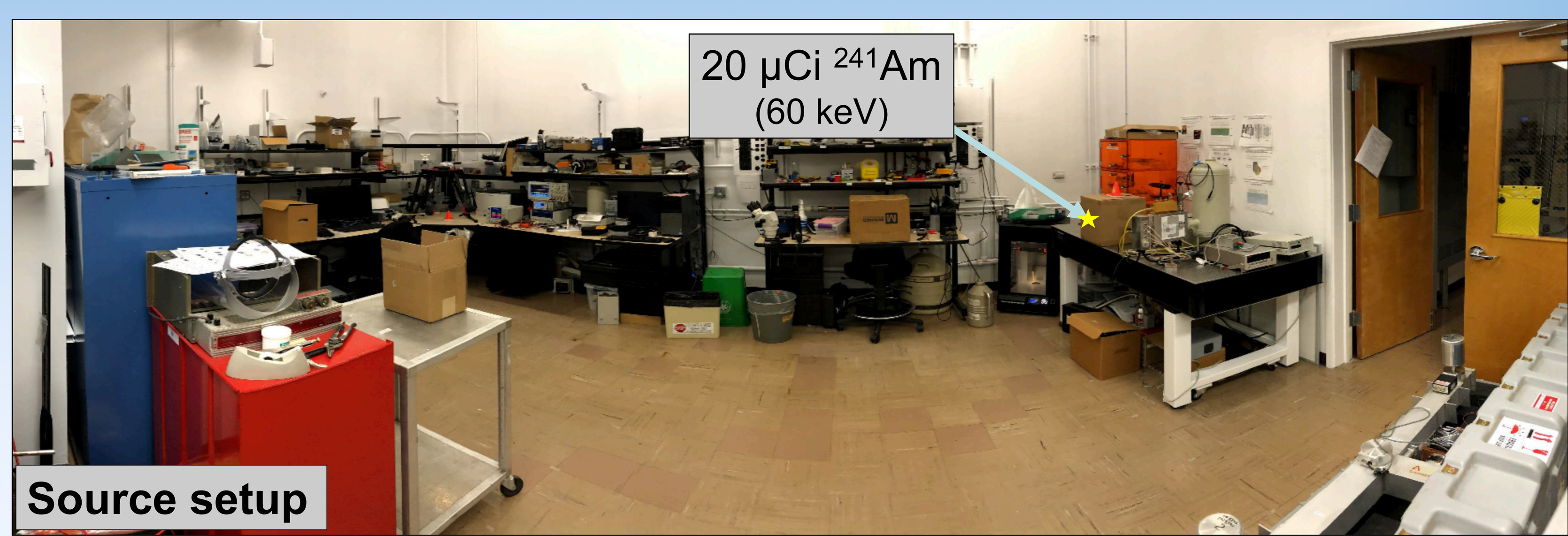

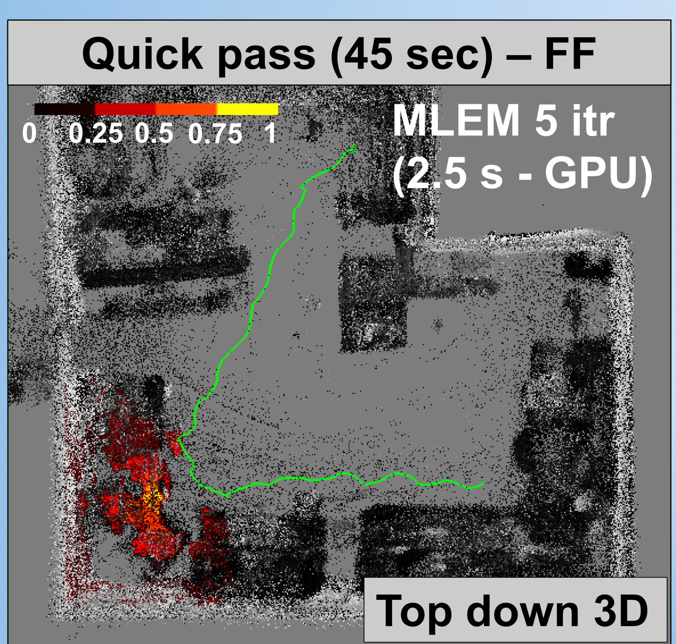

- The far-field with finite detector approximation can accurately localize, but reconstruction is noisy.
- The near-field response removes noise, but currently requires longer computation.

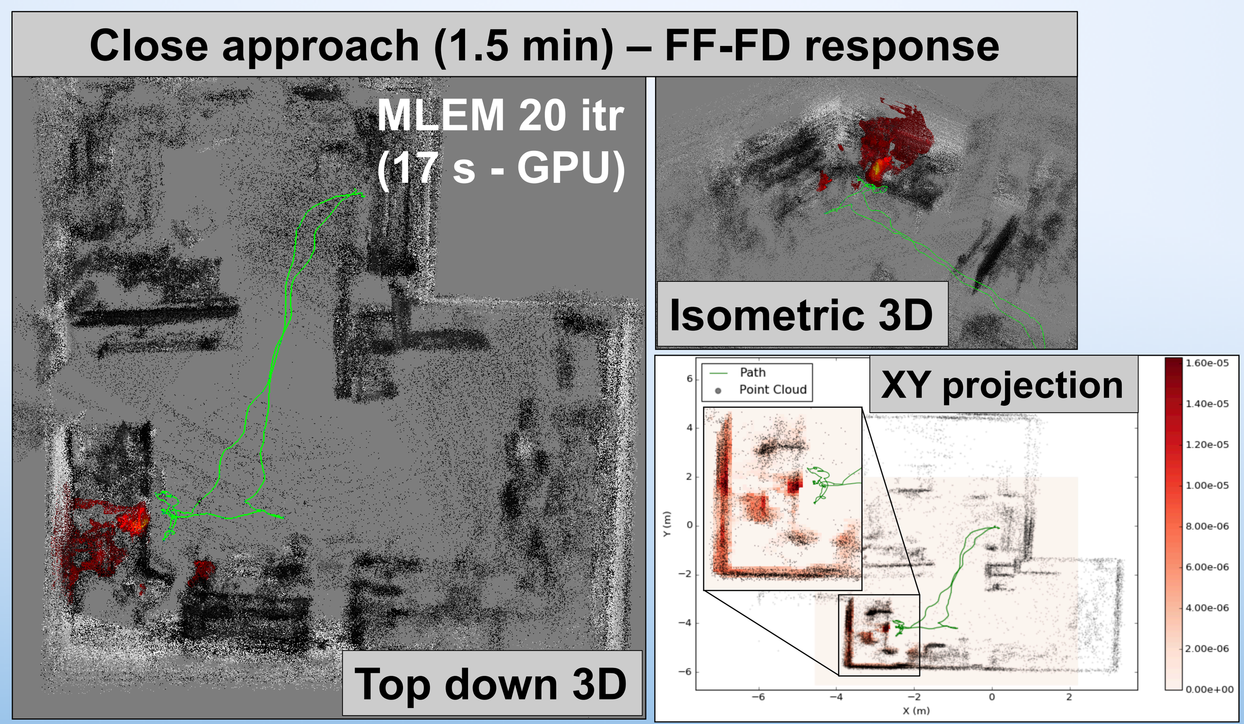

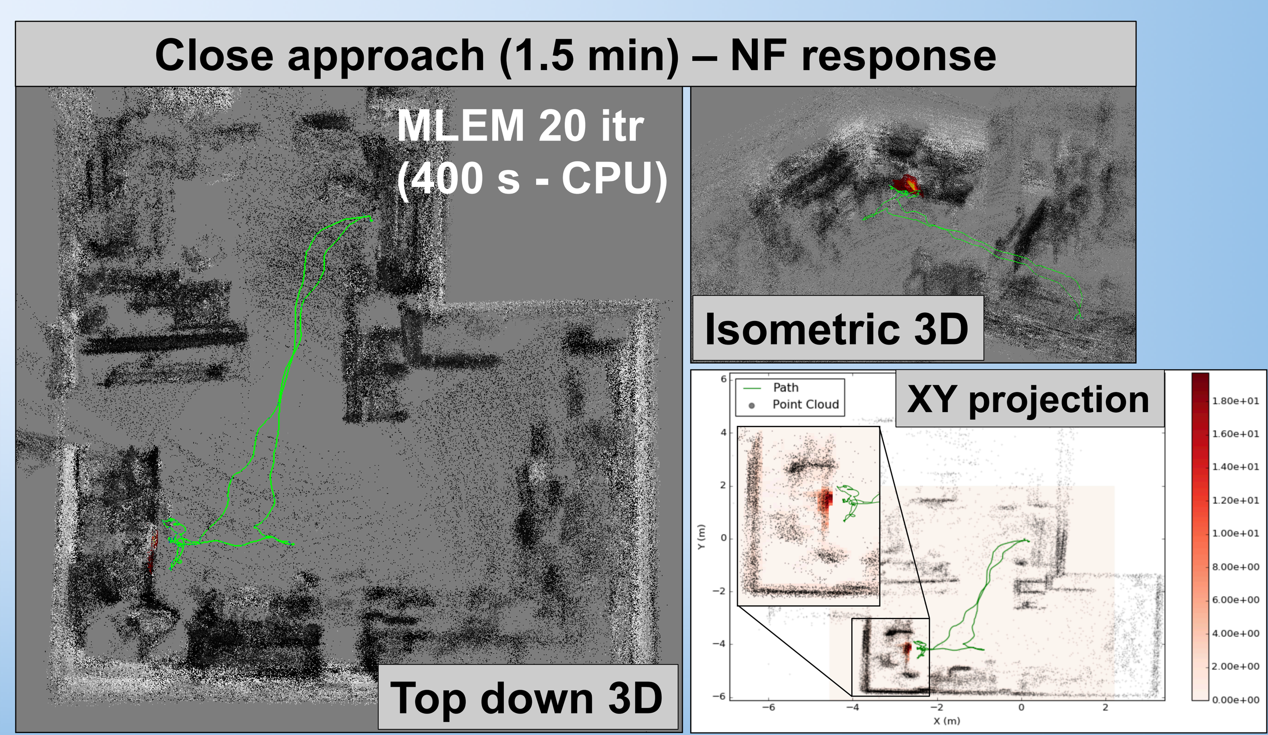

FUTURE WORK

- Development and construction of new PRISM prototype - including complete redesign of electronics and enclosure, as well as cathode readouts and a single on-board computer for contextual and gamma-ray data processing.
- Cathode readouts facilitate depth-of-interaction (DOI) and should improve imaging performance.
- Near-field reconstruction on GPU.
- Octree voxelization representation for tri-state occupancy (occupied, unoccupied, unknown).
- Adaptive non-uniform voxelization schemes.

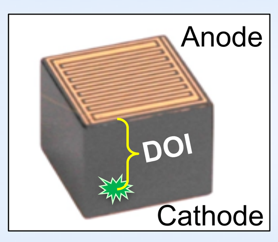

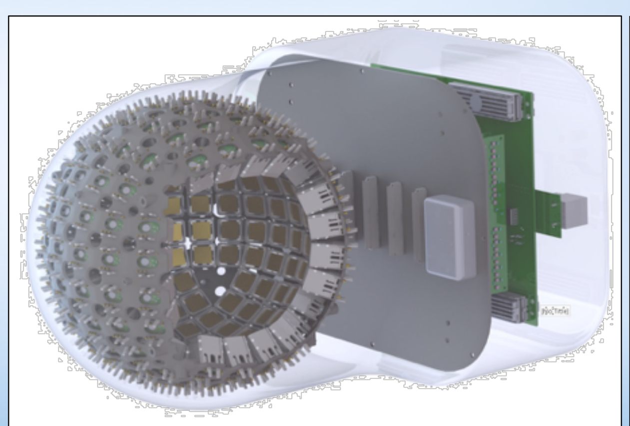
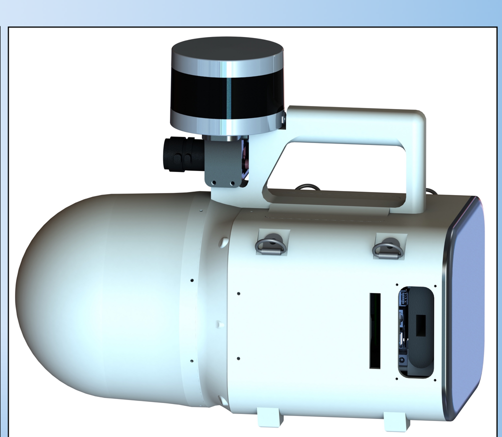

REFERENCES

[1] A. Haefner et al., Nucl. Instrum. Methods A, vol. 857, pp. 42-49, 2017.
[2] D. Hellfeld et al., IEEE Trans. Nucl. Sci., vol. 64, no. 11, pp. 2837-2842, 2017.
[3] A. P. Dempster et al., J. of the Royal Stat. Soc. B, vol. 39, no. 1, pp. 1-38, 1977.
[4] K. Khoshelham et al., Sensors, vol. 12. pp. 1437-1454, 2012.

ACKNOWLEDGEMENTS/DISCLAIMER

This material is based upon work supported by the Department of Energy National Nuclear Security Administration under Award Number DE-NA0003180 and by the Department of Defense, Defense Threat Reduction Agency under Award Number HDTRA1826768.